Raman scattering in the two-dimensional antiferromagnet $MnPSe_3$

1993 J. Phys.: Condens. Matter 5 623

(http://iopscience.iop.org/0953-8984/5/5/013)

J. Phys.: Condens. Matter 5 (1993) 623–632. Printed in the UK

Raman scattering in the two-dimensional antiferromagnet $MnPSe_3$

Chisa Makimura†, Tomoyuki Sekine†, Yoshiko Tanokura† and Koh Kurosawa‡

† Department of Physics, Sophia University, 7-1 Kioi-cho, Chiyoda-ku, Tokyo 102, Japan
‡ Department of Electrical Engineering, Miyazaki University, Miyazaki 889-21, Japan

Received 18 September 1992

Abstract. Raman spectra of the two-dimensional antiferromagnet $MnPSe_3$ are measured in the temperature region between 18 and 297 K. Below $T_N = 74 \pm 2$ K an anomalous enhancement of some Raman-active phonon peaks is observed. A new phonon peak appears below T_N at 86 cm^{-1}. The relation between its behaviour and the magnetic ordering is explained in terms of the spin-dependent phonon Raman process. A peak at 133 cm^{-1} ($T = 18$ K) shifts to low frequency with increasing temperature and disappears above T_N. It is assigned to a one-magnon Raman peak.

1. Introduction

Recently, considerable attention has been directed towards the two-dimensional (2D) antiferromagnetic system in which magnetic fluctuations are expected to be large. The MPX_3 (M = transition metal, X = S or Se) compounds show 2D properties because of their layered structure (Brec 1986). The structure of the manganese phosphorus triselenide $MnPSe_3$ derives from the CdI_2 structure. It can be described as a succession of sandwiches composed of two layers of selenium atoms between which metals and pairs of phosphorus atoms are located (see figure 1). The sandwiches are weakly bonded by the van der Waals interaction, indicating 2D structural and electrical properties. The selenium planes are stacked exactly along the c axis in an ABAB sequence, and the corresponding space group is $R\bar{3}$ (Bernasconi *et al* 1988, Wiedenmann *et al* 1981).

In $MnPSe_3$ antiferromagnetic ordering occurs in the layers below the Néel temperature $T_N = 74 \pm 2$ K (Wiedenmann *et al* 1981). The interlayer exchange interaction between the spins is much weaker than the intralayer one. Therefore, $MnPSe_3$ has magnetically a 2D structure. In the antiferromagnetic phase each Mn^{2+} ion, which is arranged in a honeycomb lattice in the paramagnetic phase, is antiferromagnetically coupled in a layer (see figure 2). The magnetic moments lie within the basal layer plane. This magnetism is interpreted as a 2D Heisenberg model or XY model (Rastelli *et al* 1979).

As a probe of magnetic properties and dynamical critical properties of spins in the magnetic materials, Raman scattering has been studied by observing not only one-magnon and two-magnon spectra but also spin-dependent phonon spectra. In

0953-8984/93/050623+10$07.50

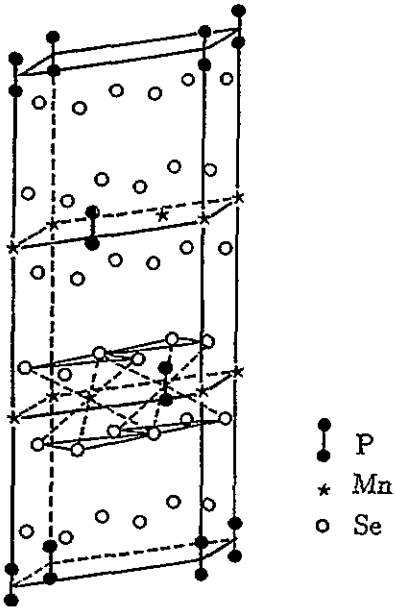

Figure 1. Crystal structure of $MnPSe_3$.

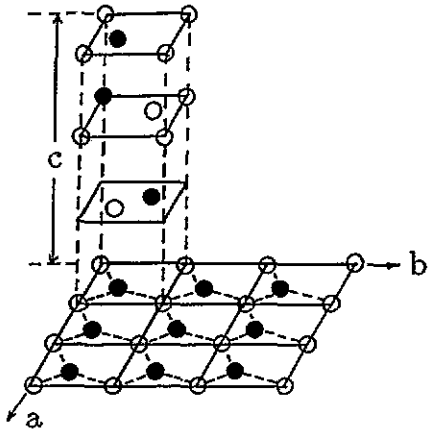

Figure 2. Magnetic structure of $MnPSe_3$ (●, atomic spins up; ○, atomic spins down).

particular the two-magnon Raman scattering gives information on the magnon–magnon interaction, because its spectrum could not be understood within the framework of a simple theory of non-interacting magnons.

On the other hand, the effect of magnetic ordering on the temperature dependence of phonon Raman intensities was first observed in the ferromagnetic semiconducting spinels $CdCr_2S_4$ and $CdCr_2Se_4$ (Steigmeier *et al* 1970). It was found that certain lines of particular symmetry, due to Raman-active phonon modes, exhibit an abrupt decrease in the integrated intensity with increasing temperature up to the Curie temperature T_C. A theory of the spin-dependent phonon Raman scattering in magnetic crystals has been developed by Suzuki and Kamimura (1972, 1973) and the spin-dependent part of the integrated Raman intensity is proportional to the square of the nearest-neighbour spin correlation. They have proposed two types of microscopic spin-dependent scattering mechanism, the variation of the d electron transfer with lattice vibrations and that of the non-diagonal exchange interaction. Many experimental studies of spin-dependent Raman scattering have since been done in europium calcogenides in which the localized f electrons play an important role in the spin-dependent Raman process (Mauger and Godart 1986) and many theoretical studies have been reported (Safran 1980).

Spin-dependent phonon Raman scattering can be divided into three main types. One is spin-ordering enhanced Raman scattering in which the spin-dependent scattering intensity of Raman-active phonons is described by the square of the nearest-neighbour spin correlation, as formulated by Suzuki and Kamimura. The second is spin-ordering induced Raman scattering. Raman-inactive phonons at $q \simeq 0$ or those at $q \neq 0$ become observable below T_N, because the symmetry in the phonon-plus-spin system is lowered or because the superstructure in this system is formed. The third is spin-disorder induced Raman scattering. In this case a broad Raman

spectrum reflecting the one-phonon density of state can be observed because the spin fluctuations break translational symmetry.

Recently spin-dependent phonon Raman scattering was also studied in the two-dimensional antiferromagnet MPX_3. In $FePS_3$, below $T_N = 118$ K drastic changes in the intensities of Raman-active phonons were observed (Balkanski *et al* 1987, Scagliotti *et al* 1985, 1987) and the Brillouin-zone-boundary phonons appeared because of the formation of a magnetic superstructure (Sekine *et al* 1990a, b). Above and below T_N, the spin-disorder induced Raman spectrum reflecting the two-dimensional one-phonon density of states of acoustic modes was found. The intensity showed a maximum at T_N, reflecting the critical phenomenon. Similarly a quasi-elastic component due to the magnetic critical scattering was first observed (Sekine *et al* 1990a, b). In $FePS_3$ the spin fluctuations are strong and they play an important role in the critical phenomena, which is probably due to the two dimensionality.

$FePS_3$ is an Ising-type antiferromagnet, while $MnPSe_3$ is a 2D Heisenberg-type or XY-type one and shows a different magnetic structure. It is interesting to compare the Raman spectra of these antiferromagnets, in particular for spin fluctuations. Also, we want to ascertain whether the theory of Suzuki and Kamimura is valid or not in the MPX_3 system where the magnetic moments originate from the spins of d electrons. Mathey *et al* (1980) reported the Raman spectra of $MnPSe_3$, but they did not observe the effect of the magnetic ordering on the Raman spectra. In this paper we report and discuss Raman scattering in the 2D Heisenberg- or XY-type $MnPSe_3$ around the magnetic phase transition.

2. Experimental details

The Raman-scattering measurements were carried out on manganese phosphorus triselenide $MnPSe_3$ single crystals. The Raman spectra were excited by the Ar^+ ion laser line (514.5 nm) in a quasibackscattering geometry with the laser beam at Brewster-angle incidence. To avoid sample heating by the laser beam, only a few tens of milliwatts were used in these experiments. The scattered light was dispersed by a Jobin–Yvon U1000 double-grating monochromator and detected by a photon counting system. The resolution of the monochromator was about 3 cm^{-1}. The samples were placed on the copper sample holder in a variable-temperature cryostat. The temperature was measured by a Pt–Co resistance thermometer and controlled within ± 0.1 K. The temperature of the samples was varied from 18 K to room temperature.

3. Results and discussion

Raman spectra of $MnPSe_3$ at room temperature and at 18 K are shown in figure 3. They show four clear peaks in the 140–250 cm^{-1} frequency region and a few weak peaks in the low-frequency region. Experiments with parallel and cross polarizations were carried out too, and the spectra are shown in figure 4. X denotes the a axis or the b axis, and Y is perpendicular to the X on the basal layer plane. The peak frequencies and the polarization characteristics are shown in table 1.

The vibrational modes of $MnPSe_3$ are shown in table 2. The symmetry of the single crystal $MnPSe_3$ is C_{3i} ($R\bar{3}$). The long-wavelength vibrations can be classified as

Table 1. Raman lines (cm^{-1}) of $MnPSe_3$ at 297 and 18 K. The representations in the parentheses are written in the case of D_{3d} layer symmetry.

297 K	18 K	Polarization	Assignment
220	222	XX	$A_g(A_{1g})$
173	175	XX XY	$E_g(E_g)$
155	157	XX XY	$E_g(E_g)$
147	149	XX	$A_g(A_{1g})$
	133	XX XY	magnon
113	112	XX XY	$E_g(E_g)$
	86	XX XY	$E_g(E_g)$
78	77	XX	$A_g(A_{2g})$

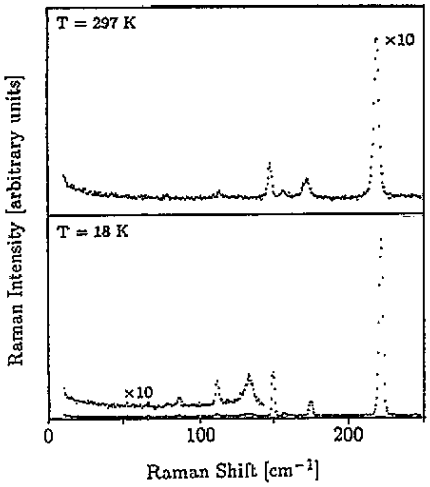

Figure 3. Raman spectra of $MnPSe_3$ recorded at 297 and 18 K, excited by the 514.5 nm line. The polarization configuration is XX.

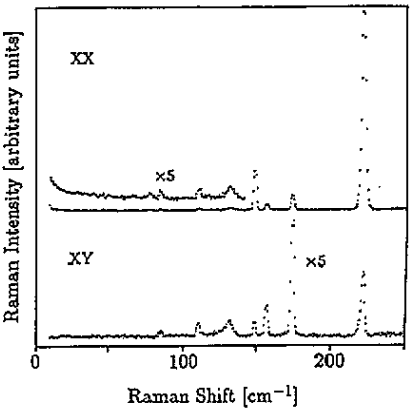

Figure 4. Polarized Raman spectra of $MnPSe_3$ at 18 K, excited by the 514.5 nm line.

$\Gamma = 5A_g + 5E_g + 5A_u + 5E_u$. Five A_g and five E_g modes are Raman active, four A_u and four E_u modes are infrared active, and an A_u and an E_u mode are acoustic. A single layer has D_{3d} symmetry in the virtual structure with ideal stacking of sandwiches. In this case, the vibrations can be classified as $\Gamma = 3A_{1g} + 2A_{2g} + A_{1u} + 4A_{2u} + 5E_g + 5E_u$. The correlations between them are shown in table 2.

Table 2. The vibrational modes of $MnPSe_3$.

Site symmetry		Crystal (C_{3i})	Layer (D_{3d})
$P_2Se_6(C_{3i})$	$4A_g$	$5A_g$	$3A_{1g}$
			$2A_{2g}$
	$4E_g$	$5E_g$	$5E_g$
	$4A_u$	$5A_u$	A_{1u}
			$4A_{2u}$
	$4E_u$	$5E_u$	$5E_u$
$2Mn(C_3)$	2A		
	2E		

On the basis of the present experiment and previous analyses (Scagliotti *et al* 1987, Mathey *et al* 1980), the Raman peaks can be assigned as follows. The intense peak at 222 cm^{-1} ($T = 18$ K) is strongly polarized. It is assigned to the A_g mode of the P_2Se_6 group which comes from the symmetric stretching vibration of the P–Se bonds. The 175 cm^{-1} and 157 cm^{-1} peaks ($T = 18$ K) are depolarized. They are assigned to E_g modes. The 149 cm^{-1} peak ($T = 18$ K) is polarized and can be assigned to an A_g mode. The previous studies showed that the cation-substitution effect was observed mainly below about 140 cm^{-1} in the infrared and Raman spectra of the transition-metal phosphorus trichalcogenides (Scagliotti *et al* 1987, Mathey *et al* 1980). Therefore, the peaks in the low-frequency region can be assigned to vibrational modes which involve mainly the vibrations of the metal cations. A peak at 77 cm^{-1} was observed in the XX polarization, as shown in figure 4. Its intensity becomes weak at low temperature, so that we sometimes could not detect it. This is assigned to an A_g mode which would be a Raman-inactive A_{2g} mode in the D_{3d} symmetry (Bernasconi *et al* 1988).

The Raman spectra of $MnPSe_3$ crystals at room temperature and at 18 K are compared in figure 3. The peaks shift slightly towards higher frequency as the temperature is lowered and the most attractive change is observed in Raman intensities of these peaks. So we measured Raman spectra at various temperatures, and plotted the intensities as a function of temperature.

The Raman spectrum may be described by a spectral function,

$$I(\omega) = k^2(n(\omega)+1)2\omega\gamma/[(\omega_0^2-\omega^2)^2+4\omega^2\gamma^2] + \text{BG} \tag{1}$$

where ω_0, γ, and k are the phonon frequency, the damping constant, and the coupling coefficient of the phonon for the photon, respectively. $n(\omega)$ is the Bose factor, and BG is the background. The integrated intensity is given as

$$I = \int_0^\infty [I(\omega) - \text{BG}]\,\mathrm{d}\omega \sim (n(\omega_0)+1)k^2\pi/2\omega_0. \tag{2}$$

Then the square of the coupling coefficient k^2 is proportional to the integrated intensity divided by the population factor. The ratios of $k^2(T)/k^2(18\text{ K})$ of the 222, 175 and 149 cm^{-1} peaks are shown in figure 5. It is shown that the intensities increase abruptly below $T_N = 74$ K. This relates clearly to the magnetic ordering.

A general theory of the spin-dependent phonon Raman scattering in magnetic crystals has been developed by Suzuki and Kamimura (1972, 1973). They have derived the following expression for the integrated phonon Raman scattering intensity $I(T)$ as a function of temperature T

$$I(T) = (n(\omega_0)+1)\left\{\left|R + M\frac{\langle S_0 \cdot S_1\rangle}{S^2}\right|^2 + |K|^2\langle S_z\rangle^2\right\} \tag{3}$$

where the first term represents the spin-independent part and the second one the spin-dependent part which is proportional to the nearest-neighbour spin correlation function. The coefficients R, M and K are temperature independent. Both the modulation of the d electron transfer energy and that of the non-diagonal exchange interaction by the lattice vibration can contribute to the second term. But Suzuki

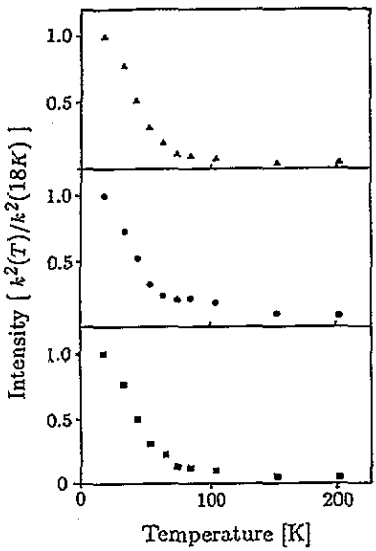

Figure 5. Temperature dependence of $k^2(T)/k^2(18\ \mathrm{K})$ of the peaks at 149 cm^{-1}(▲), 175 cm^{-1} (●) and 222 cm^{-1} (■) in the spectra of $MnPSe_3$.

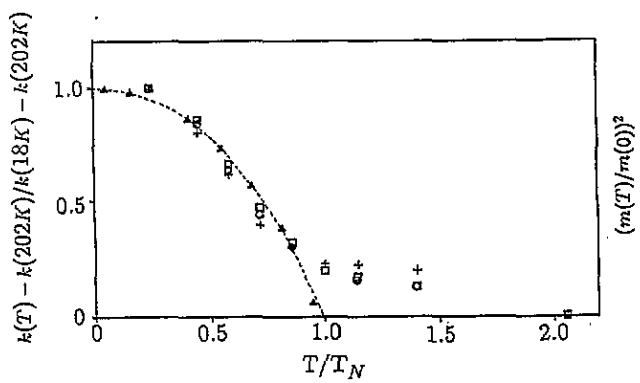

Figure 6. Comparison of $k(T)$ of the 149 cm^{-1}(□), 175 cm^{-1} (+) and 222 cm^{-1} (○) lines, in the spectra of $MnPSe_3$ with the square of the reduced magnetization $(m(T)/m(0\ \mathrm{K}))^2$ (▲) (Wiedenmann *et al* 1981).

and Kamimura pointed out that the former is essentially important in $CdCr_2Se_4$ and $CdCr_2S_4$. The last term is associated with the spin–orbit interaction with relative displacements of ions. K is shown to be one or two orders of magnitude smaller than R and M and therefore it can be disregarded (Suzuki and Kamimura 1973). By removing the effect of the Bose factor, we obtain

$$k^2(T) \propto \left| R + M \frac{\langle S_0 \cdot S_1 \rangle}{S^2} \right|^2 . \tag{4}$$

In the high-frequency phonons of $MnPSe_3$, the patterns of $k^2(T)$ correspond to the range of $R/M < 0$, judging from figure 5. We considered that k^2 at 202 K comes mainly from the spin-independent part R, and then we obtain

$$k(T) - k(202\ \mathrm{K}) \propto |\langle S_0 \cdot S_1 \rangle|. \tag{5}$$

In figure 6 we plotted the values of $[k(T)-k(202\ \mathrm{K})]/[k(18\ \mathrm{K})-k(202\ \mathrm{K})]$ obtained from the peaks at 149, 175 and 222 cm^{-1}.

In the molecular-field approximation, $\langle S_0 \cdot S_1 \rangle$ can be expressed as (Callen 1968)

$$\langle S_0 \cdot S_1 \rangle \propto m^2(T) \tag{6}$$

where $m(T)$ is the sublattice magnetization in the antiferromagnets. In this case the short-range ordering is completely neglected. Wiedenmann *et al* (1981) obtained the reduced magnetic moment by neutron diffraction measurement. The data are plotted in figure 6. Far below T_N the agreement between $k(T) - k(202\ \mathrm{K})$ and $m^2(T)$ is good but near T_N it becomes worse because the short-range ordering of the nearest-neighbour spin correlation becomes strong. However, except for near T_N, the agreement is relatively good, suggesting that the spin fluctuations are weak.

The temperature dependence of the Raman spectrum of $MnPSe_3$ in the low-frequency region is shown in figure 7. Three peaks can be observed at 27 K. As mentioned above, the 77 cm^{-1} peak was not observed in this figure. The 86 cm^{-1} peak disappears above T_N. Its coupling coefficient k obtained by equation (1) is shown in figure 8. In europium calcogenides, the Raman-inactive LO phonon at $q \simeq 0$ was observed under the resonant condition for the incident light in the ferromagnetic phase. This becomes Raman active in the ferromagetic phase on the electric-dipole–electric-quadrupole process (Safran *et al* 1976, 1977, Güntherodt 1979). In the present case the symmetry of the lattice-plus-spin system is not lowered in the antiferromagnetic phase shown in figure 2. Since it is not an LO phonon judging from the data of the infrared spectroscopies (Mathey *et al* 1980, Kliche 1984), the electric-dipole–electric-quadrupole process cannot be considered. In principle ten Raman peaks should be seen, but only six peaks can be detected at room temperature. We assigned the 86 cm^{-1} peak to an originally Raman-active E_g mode because of its polarization characteristic.

In this case $R \simeq 0$ holds in equation (4). We fit the coupling coefficient k of the 86 cm^{-1} peak with the square of the reduced magnetic moment obtained by the neutron diffraction measurement (Wiedenmann *et al* 1981). When compared with the high-frequency phonons of figure 6, the agreement between them is excellent, because the short-range ordering of the nearest-neighbour spin correlation was originally so weak that its signal was below the detectable level in this case.

The magnetic moment of $MnPSe_3$ originates from the d electron of a magnetic ion Mn^{2+} with a spin of $\frac{5}{2}$. The circumstances correspond to the model of Suzuki and Kamimura. In contrast the localized f electrons play this role in europium calcogenides, in which the spin–orbit interaction is important (Güntherodt 1979). In the theory of Suzuki and Kamimura, during the process where a d electron in a transition-metal ion transfers to the neighbouring ion via the intervening non-magnetic ions, a phonon is created or destroyed by the d-electron–phonon interaction. In particular the phonons, in which the non-magnetic ions are strongly vibrating, are easily created or destroyed in this process. In $MnPSe_3$ the high-frequency phonons

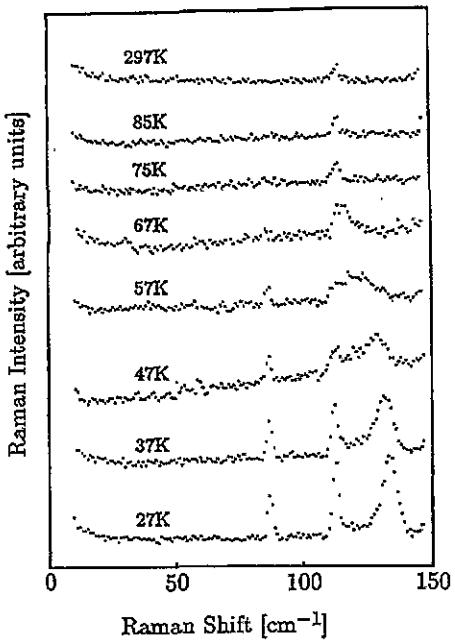

Figure 7. Temperature dependence of Raman spectra of $MnPSe_3$ in the low-frequency region. The polarization configuration is $YX + YY$.

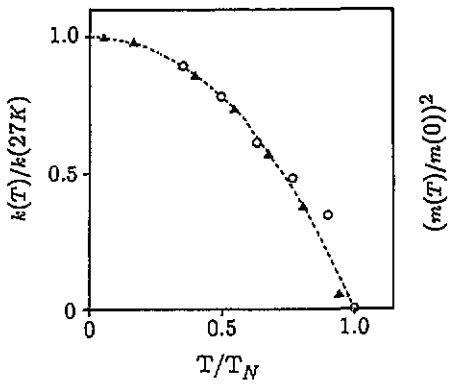

Figure 8. Comparison of $k(T)/k(27\ \mathrm{K})$ of the 86 cm^{-1} line (○) in the spectrum of $MnPSe_3$ with the square of the reduced magnetization $(m(T)/m(0\ \mathrm{K}))^2$ (▲).

come from the internal vibrations of the P_2Se_6 molecule and the spin-dependent term is much stronger than the spin-independent term. We, therefore, think that this is an ideal system for the model of Suzuki and Kamimura. In the 86 cm^{-1} peak the P_2Se_6 molecule is probably vibrating strongly although the magnetic ions are vibrating.

On the other hand on the 77 cm^{-1} peak and the 112 cm^{-1} peak the spin-dependent effect is weak, as shown in figure 9. In their normal coordinates, the magnetic ions are strongly vibrating, while the movements of the non-magnetic atoms are probably small. The peak at 133 cm^{-1} ($T = 27$ K) shifts to low frequency and its intensity decreases with increasing temperature, and apparently vanishes for temperatures in excess of $T_N = 74$ K (see figure 9). The half widths of the peaks at 133 cm^{-1} and 112 cm^{-1} are shown in figure 9. The line width of the 133 cm^{-1} peak becomes broad and diverges with increasing temperature towards T_N. From this behaviour we consider that this peak is due to one-magnon scattering.

4. Conclusions

The Raman spectra of manganese phosphorus triselenide $MnPSe_3$ show four clear peaks in the frequency region between 140 and 250 cm^{-1}, and a few weak peaks in the low-frequency region. The four clear peaks show enhancement of the intensity below $T_N = 74 \pm 2$ K. A comparison of the intensity enhancement with the theory of the spin-dependent phonon Raman scattering formulated by Suzuki and Kamimura (1972, 1973) shows good agreement. In the low-frequency region, a new phonon peak

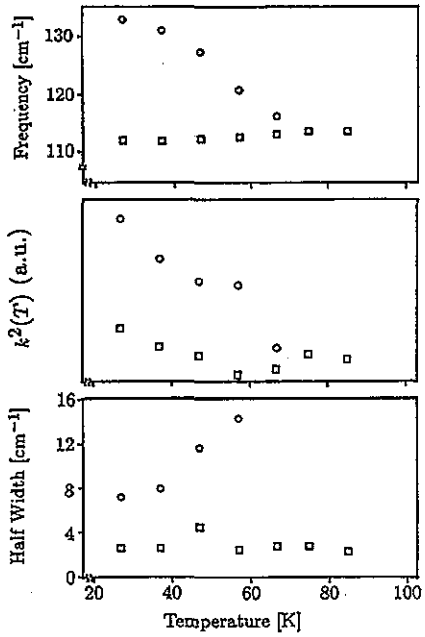

Figure 9. Temperature dependence of the frequencies ω_0, of $k^2(T)$ and of the half widths 2γ of the peaks, at 133 cm^{-1} (○) and 112 cm^{-1} (□) in $MnPSe_3$.

appeared at 86 cm^{-1} (T = 18 K). It is assigned to an originally Raman-active E_g phonon and the intensity is also explained by the theory of Suzuki and Kamimura.

A peak at 133 cm^{-1} shifts to low frequency and the intensity decreases with increasing temperature, and it cannot be observed above T_N. This is Raman scattering from one magnon.

In contrast with the Ising-type antiferromagnet $FePS_3$, we were not able to find the effect of the spin fluctuations on Raman spectra of the 2D-Heisenberg-type or XY-type $MnPSe_3$ since they are weak. It is probably consistent with the fact that the nearest-neighbour spin correlation is approximately proportional to the square of sublattice magnetization in $MnPSe_3$ since the short-range ordering is weak.

References

Balkanski M, Jouanne M, Ouvrard G and Scagliotti M 1987 *J. Phys. C: Solid State Phys.* **20** 4397
Bernasconi M, Marra G L, Benedek G, Miglio L, Jouanne M, Julien C, Scagliotti M and Balkanski M 1988 *Phys. Rev.* B **38** 12089
Brec R 1986 *Solid State Ionics* **22** 3
Callen E 1968 *Phys. Rev. Lett.* **20** 1045
Güntherodt G 1979 *J. Magn. Magn. Mater.* **11** 394
Kliche G 1984 *J. Solid State Chem.* **51** 118
Mathey Y, Clement R, Sourisseau C and Lucazeau G 1980 *Inorg. Chem.* **19** 2773
Mauger A and Godart C 1986 *Phys. Rep.* **141** 51
Rastelli E, Tassi A and Reatto L 1979 *Physica* B **97** 1
Safran A S 1980 *J. Physique Coll.* **5** 223
Safran A S, Dresselhaus G, Dresselhaus S M and Lax B 1977 *Physica* B **89** 229
Safran A S, Lax B and Dresselhaus G 1976 *Solid State Commun.* **19** 1217
Scagliotti M, Jouanne M, Balkanski M and Ouvrard G 1985 *Solid State Commun.* **54** 291
Scagliotti M, Jouanne M, Balkanski M, Ouvrard G and Benedek G 1987 *Phys. Rev.* B **35** 7097
Sekine T, Jouanne M and Balkanski M 1990a *J. Magn. Magn. Mater.* **90 & 91** 315
Sekine T, Jouanne M, Julien C and Balkanski M 1990b *Phys. Rev.* B **42** 8382

Steigmeier F E and Harbeke G 1970 *Phys. Kondens. Materie* **12** 1
Suzuki N and Kamimura H 1972 *Solid State Commun.* **11** 1603
—— 1973 *J. Phys. Soc. Japan* **35** 985
Wiedenmann A, Rossat-Mignod J, Louisy A, Brec R and Rouxel J 1981 *Solid State Commun.* **40** 1067